

APPLICATION OF RENEWABLE ENERGY SOURCES IN
CATHODIC PROTECTION AND THEIR ECONOMICAL ASPECTS

M.G. Osman
College of Engineering, El-Mansoura University,
El-Mansoura, Egypt.

ABSTRACT:

As cathodic protection systems are fed from D.C. sources, a difficulty will be faced to find a suitable D.C. source if such systems are used to protect petroleum tanks or pipe lines which lie in isolated areas far away from the existing transmission lines. Usually 3 methods could be adopted here:

i) Installing a transmission link with a rectifier substation between the nearest convenient existing transmission line and the D.C. cathodic protection source.

ii) Using private motor-generator sets; where the motor as a prime mover works by convenient fossil fuel.

iii) Using storage battery systems, the capacity of which must be large enough to supply the required protective current during a period necessary for charging a second battery at the nearest charging station and replacing the one in use. In this case the charging battery system may be fed from rectifier substations, or private D.C. generating sets whose prime movers operate with conventional or non-conventional energy sources.

This paper presents the limitations and conditions required for the conveniency of applying the non-conventional energy sources (photovoltaic) and their economical aspects in charging such batteries; together with examples of calculations clarifying the analytical steps and assumptions adopted in this study by means of which the final conclusions and results presented here were deduced. A simplified approach for the solar specific annual energy cost calculations using nomogram analysis and performance charts applied to local conditions in this respect is presented also in this paper.

INTRODUCTION:

Figure (1) represents the wiring diagram, and the main components of a cathodic protection system fed from an existing 11 K.V. transmission line 1; which is connected to the transformer 2, stepping down the voltage so as to be suitably connected to the rectifier 3. The output of the rectifier is the D.C. source for the cathodic protection system, the positive terminal "X" of the D.C. source is connected through the distribution line 4, and the anode electrode group 6 through the regulating resistance 5; while the negative terminal "y" of the D.C. source is connected to the pipe line required to be protected. In isolated areas; where the metallic installations required to be protected are far away from the existing transmission lines; the cost of installing a transmission link between

source of the protective system together with the cost of the transformer 2 and the rectifier 3 will be some what expensive. In order to overcome this difficulty, the following solutions have been suggested (1), (2)

1) The cathodic protection installation could be powered by an internal combustion engine which drives a D.C. generator as shown in Fig. 2.

11) Using storage battery systems especially when the required power rating is relatively small; the capacity of which must be large enough to supply the required protective current during a period necessary for charging a second battery at the nearest charging station, and replacing the one in use. Examples for such case are shown in Fig. 3-a,b which represents the layout of a battery system charged from a mounted pole rectifier unit, so as to eliminate by this way the electrical transmission line between the existing transmission line and the main D.C. source of the cathodic protection system, and Fig. 4. Which shows a cathodic protection installation with a D.C. supply fed from a wind electric set combined with a storage battery system. According to the favourable atmospheric conditions, a photovoltaic system could substitute the wind electric set in Fig. 4 when used as a battery charging system in such application. The economical aspects and analytical studies in this respect for the proper selection of the type of the battery charging system concerning the P.V. sets are illustrated in the following items.

Power Extracted From Photovoltaic Cells:

Many studies have discussed theories and methods of relating solar cell output to parameters connected with sun's intensity. The sun's angular position w.r.t. a panel and the length of the solar day are simple functions to calculate. The solar intensity is much more difficult, requiring specifications of atmospheric aerosols, their distribution and index of refraction and also the specifications of various absorbing gases in the atmosphere. To predict the direct and diffuse solar intensity at a panel is extremely complicated. The solar plant output energy E is predicted by

$$E = T.S.G. \quad \dots(1)$$

where;

- E = Solar cell output energy
- S = Panel sensitivity factor.
- T = Tilt factor.
- G = Global energy.

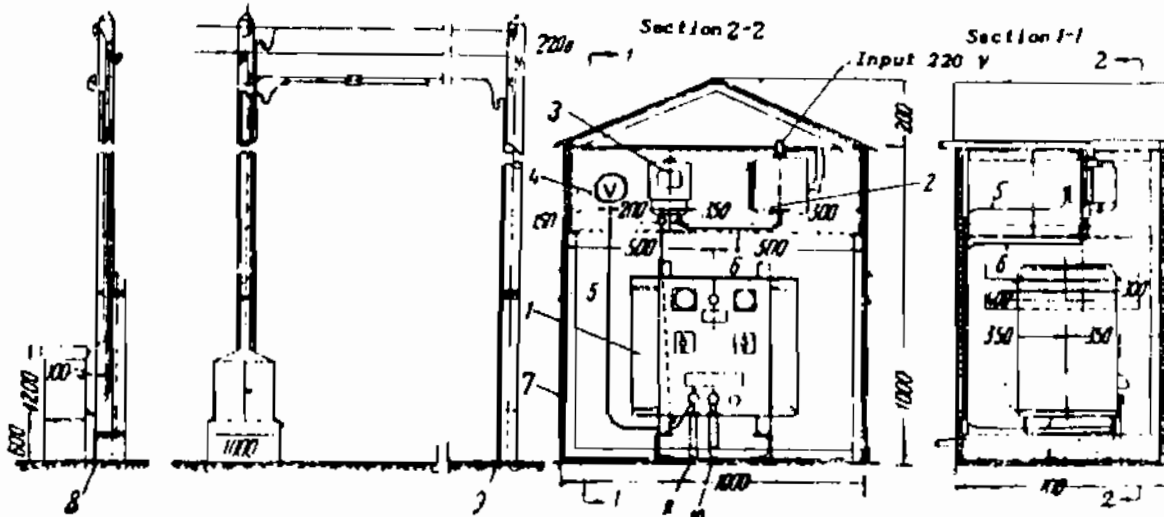
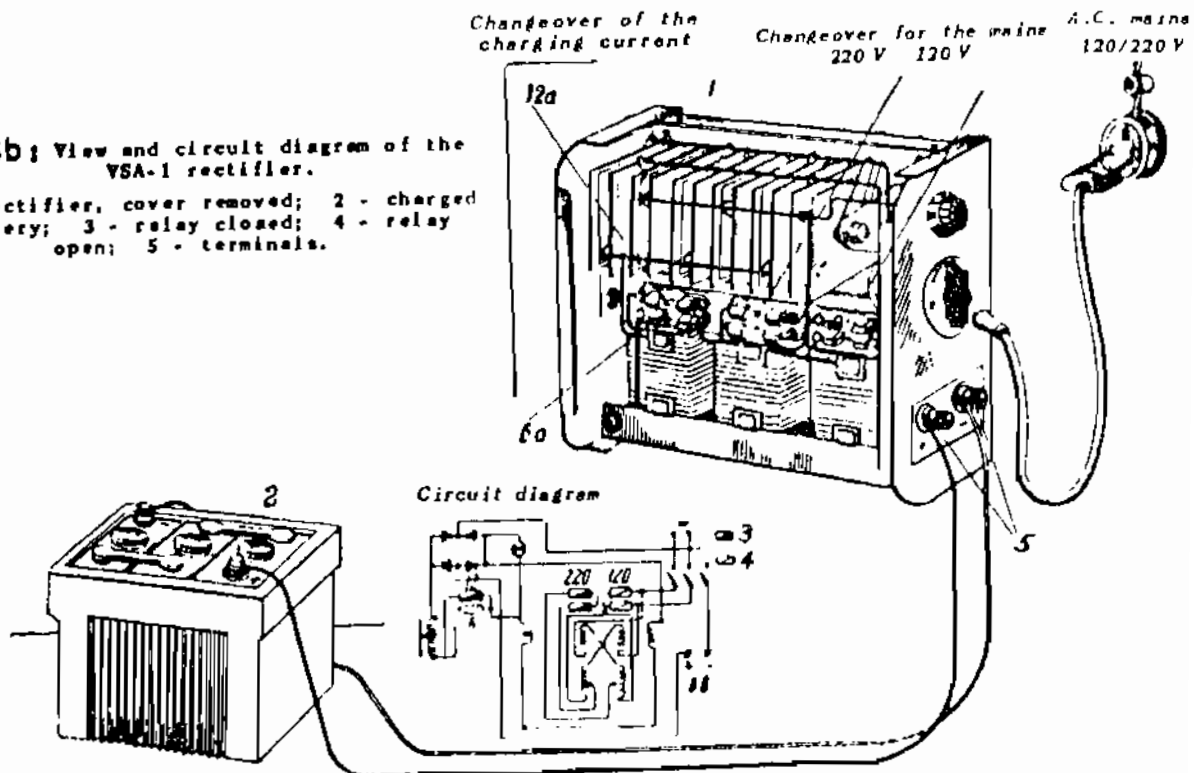


Fig. 3a: Installation of the rectifier containing box on the mast.

- 1 - rectifier; 2 - starter box; 3 - single phase meter 220 V, 10 A;
- 4 - d.c. voltmeter 0 to 30 V; 5 - 80 cable of 1 x 1.5 cross section; 6 - same, 2 x 2.5 cross section; 7 - metallic case; 8 - to anode earthing;
- 9 - to the protected pipeline; 10 - to the regulating resistance.

Fig. 3b: View and circuit diagram of the VSA-1 rectifier.

- 1 - rectifier, cover removed; 2 - charged battery;
- 3 - relay closed; 4 - relay open; 5 - terminals.



Energy balance of the P.V. plant and battery storage: (3)

The energy balance of the P.V. plant is easily obtained with the help of Fig. (5).

The total daily energy balance

$$E_A = E_p \eta_{PT} - E_G / \eta_I \quad \dots (1)$$

where E_G is daily load demand, E_A corresponding energy entering the battery. Battery state of charge changes by ΔC_B

$$\Delta C_{BA} = E_A \eta_B \quad \text{if } E_A > 0 \text{ (charging)} \quad \dots (3)$$

$$\Delta C_{BA} = E_A / \eta_B \quad \text{if } E_A < 0 \text{ (discharging)} \quad \dots (4)$$

During night the battery discharges and supplies the nightly load demand E_n .

$$\therefore \Delta C_{BN} = - E_n / \eta_D \quad \dots (5)$$

new battery state of charge = $C_B + \Delta C_{BA} + \Delta C_{BN}$ $\dots (6)$
 where:

$$C_{min} \leq C_B \leq C_{max} \text{ (limits of change)}$$

A- If C_{min} is reached \therefore deficit is recorded

$$E_D = E_G + E_n \quad \dots (7)$$

\therefore load supplied by conventional source, all P.V. is supplied to battery.

$$\Delta C_{BA} = E_p \eta_{PT} \eta_B \quad \dots (8)$$

$$\Delta C_{BN} = 0 \quad \dots (9)$$

The situation remains unchanged until the prescribed state of charge C_{max} has been restored. (C_{min} to C_{max}) Then the plant is switched again to the normal operation mode.

B- If the battery reaches the maximum charge, C_{max} , surplus is recorded.

$$E_s = E_p \eta_{PT} - E_G / \eta_I \quad \dots (10)$$

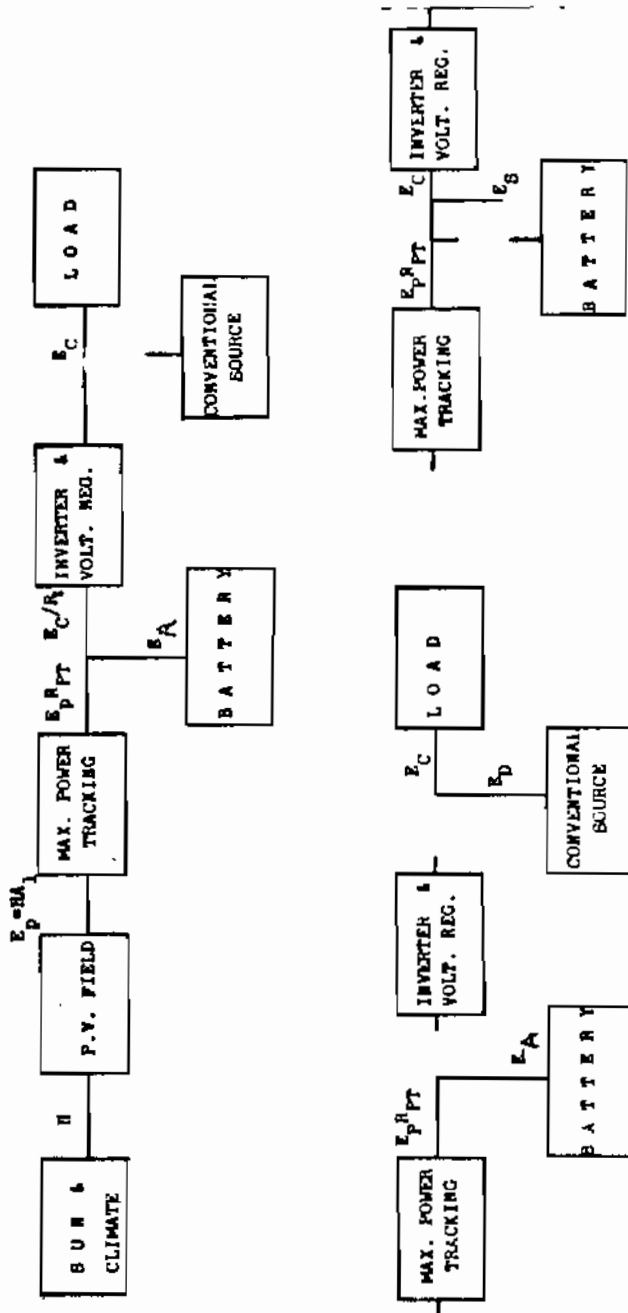


Fig. 5: Structure of the P.V. system and battery storage with the energy management logic.

This energy balance can be performed day-by-day with the help of computer, to calculate number of days the battery takes to go from one state of charge to the other.

Micro Computer Aided Solution For Energy Balance: (4)

- 1- Read input data; solar radiation /unit area $H(M)$, day and night load demand for each month: $E_g(M)$, $E_n(M)$, given for each month M .
- 2- Set surplus and deficit energies E_s and E_d to zero, define η_{pc} , η_B , η_I , and supply A_1 and C_{max} .
- 3- Set the battery C_{min} and C_{re} and the battery charge C_B to a suitable initial value ($C_B = C_{max}$) for example, and supply A_1 and C_{max} the P.V. plant components.
- 4- Point 1 in the flow chart, energy balance is started in the first month of the year ($M = 1$) by calculating separately A and B (day and total balance).
- 5- Negative balance leads to calculate N_A , the number of days to get the condition $C_B = C_{min}$. (Point 2).
- 6- If N_A exceeds days in a month. result is only up dating. C_B (charge Value), deficit is not reached (Point 5).
- 7- Other wise the number of days N_D , in which a deficit will be recorded is calculated, and the sum $N_B = N + N_D$ tested (point 6), against the number of days in the month. Two situations can occur.
 - a) $N_B \geq 30.4$ resulting in updating the C_B value to the last day of the month.
 - b) $N_B < 30.4$ resulting in restoring the battery charge to the value prescribed to switch again the PV plant to the load $C_B = C_{re}$.
- 8- Then the routine cycles again to point 2, within the same month, In both cases the deficit in energy is calculated.
- 9- If overall energy balance has been found positive, point 3, a surplus energy is recorded only if the battery gets the full charge within a single month (point 4). Other wise, the battery state of charge is just up dated.
- 10- At the end of each month some relevant quantities such as the energy balance, the battery state of charge, surplus and deficit are printed and calculation repeated starting from point 1, with the appropriate date to the next month.

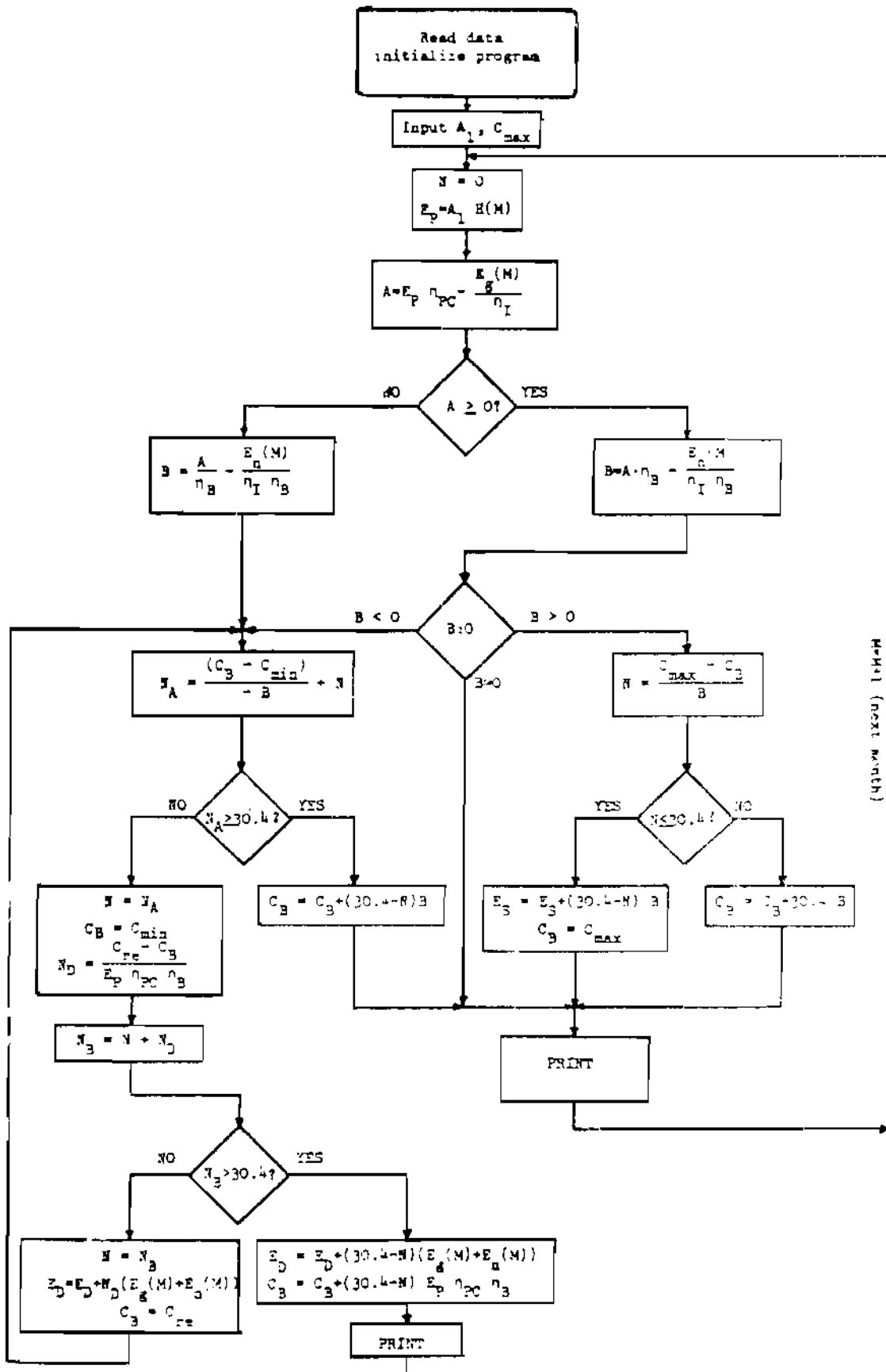


Fig. 6: Calculation of the performance $f_1(M)$ based on monthly data.

Factors Affecting the Economical Study of the P.V. System:-

The different solutions obtained by performing the energy balance of the plant for different sizes of the PV field and battery, can be displayed into a shape similar to that of Fig.(7) by plotting the energy deficit as function of normalized PV. field size, with the battery storage capability, g_p as a parameter, for certain tilt angle and constant load demand. The normalizing units are as follows: For the battery it is the max daily load demand divided by inverter efficiency times the maximum battery discharge. For the PV field it is the maximum load power divided by inverter efficiency (if any). As for the deficit normalized unit it is the yearly load demand divided by inverter efficiency (if any).

The cost of each plant configuration can be determined as follows:

- 1- The cost of the PV field is determined as a function of its size (peak power).
- 2- The cost of various items that are proportional to the PV field size are added such as PV panels support structures, land cost and electrical connections.
- 3- The cost of storage batteries including their building and maintenance cost and cost of batteries times number of battery replacements within the plant life time.
- 4- The cost of non PV systems (maximum power tracker, inverter), that can be related to the maximum power load.

Figure (8) shows the cost of the plant as a function of PV field size with constant deficit. Each curve display a minimum value corresponding to the best balance (from an economic point of view) between battery size and PV plant size. Table (1) reports some of informations that can be used to determine the above mentioned cost factors. Of course the minimum cost condition has to be balanced with other consideration as reliability of the plant that may suggest to choose a plant configuration different from that satisfying the purely economic point of view.

Table 1: Some useful data for cost analysis of PV plants.

Item	Unit cost
Photovoltaic Panels	10 \$/m ²
Purchase and preparation of site	5 \$/m ²
Storage batteries	80 \$/kWh
Electrical wiring	200 \$/km ²
Support structures	20 \$/m ²

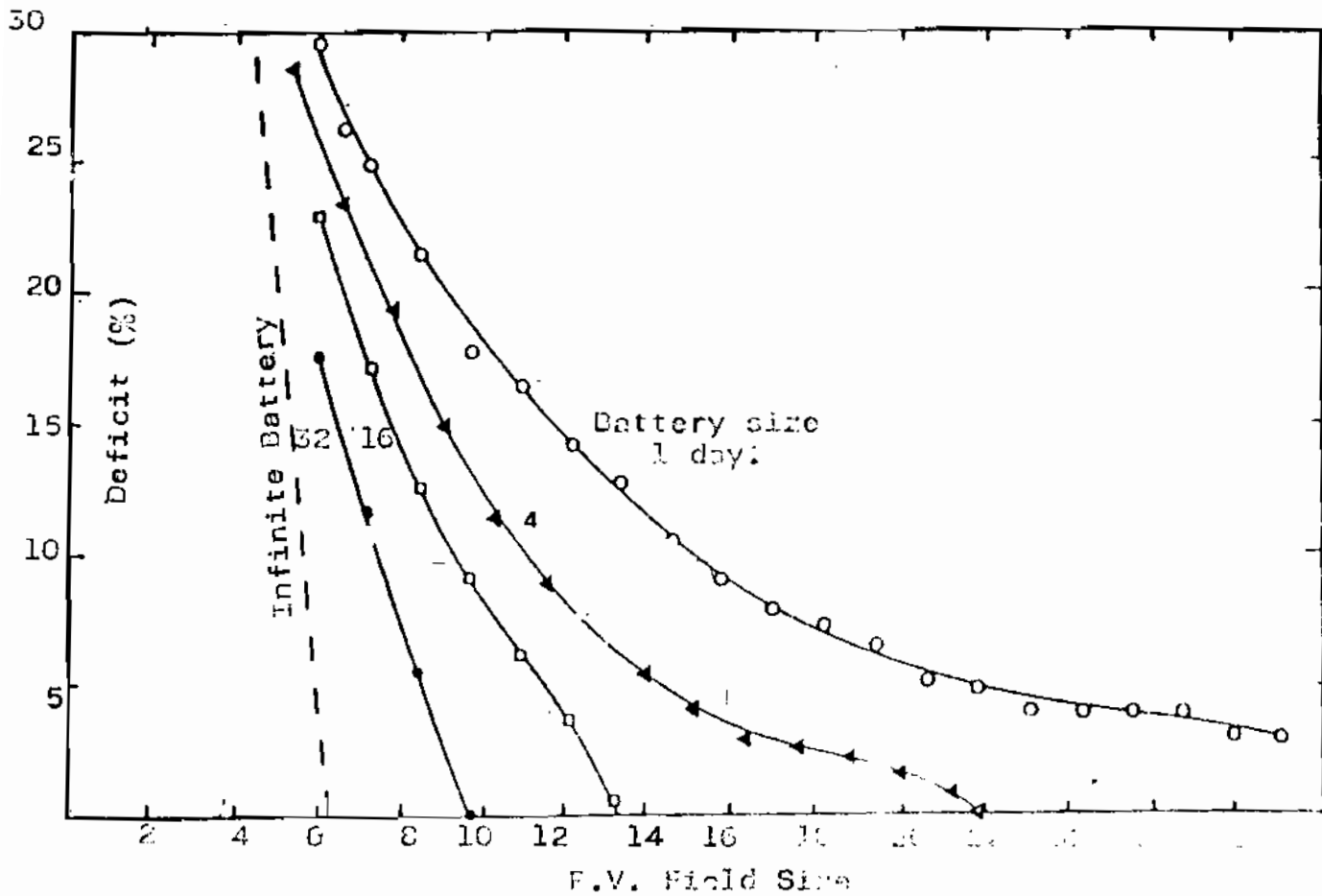


Fig.(7): Map of the deficit of the plant as a function of the F.V. field size, for different battery storage capabilities.

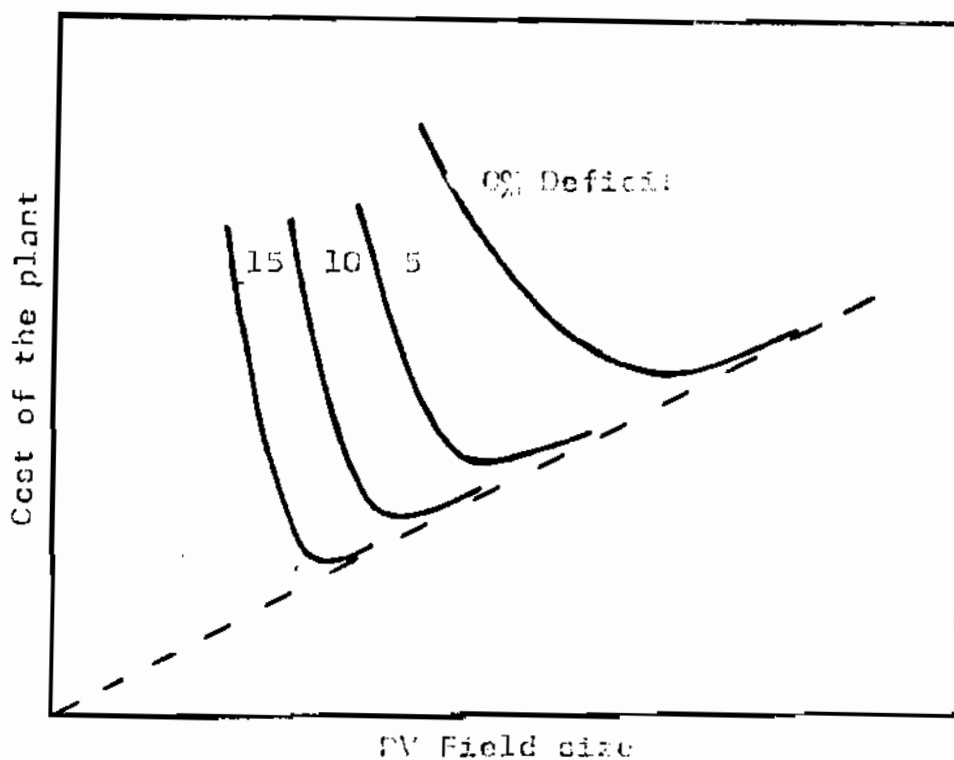


Fig.(8): Search of the minimum cost condition for the plant.

Performance of the P.V. Cell:

The current-voltage (I-V) characteristic for the illuminated junction is plotted in Fig.(9) for several different light intensities. V_{oc} (Open circuit voltage) varies only slightly with light intensity. It has been shown that the characteristic equation for an ideal P.V. cell may be expressed as:

$$I = I_{sc} - I_{sd} (e^{qV/kT} - 1) \quad \dots(11)$$

where $V_T = \frac{kT}{q}$ (V) is the thermal voltage,

k = Boltzmann constant 1.38×10^{-23} J/°K

q = electronic charge 1.6×10^{-19} C

T = Cell absolute temperature
 $= T_c + 273$ (°K)

I_{sc} = Short circuit current density at 25°C and 1 KW/m² solar radiation.

I_{sd} = The dark saturation current.

and such a cell could be represented by the simple equivalent circuit in Fig.(10). It consists of a constant current generator (for fixed light intensity) with current output equal to the optically generated current I_{sc} in parallel with the ideal dark diode which by passes some of the optically generated current to give a reduced current at the terminals. In use the cell is connected to a load which is represented by the resistance R_L .

Open circuit voltage, $V_{o.c.T}$ and short circuit current (at 1 KW/m² radiation) $I_{e.c}$ at the temperature T_c (°C) are linear functions of temperature:

$$V_{oct} = V_{oco} [1 + h_V (T_c - 25)] \quad \dots(12)$$

$$I_{scT} = I_{sco} [1 + h_I (T_c - 25)] \quad \dots(13)$$

where $h_V = -3.7 \times 10^{-3}$ 1/°C & $h_I = 6.4 \times 10^{-4}$ 1/°C

Fig.(11) shows the variation of efficiency with temperature.

The output power from the cell is the product of terminal voltage and output current, or

$$P = VI = V \left\{ I_{sc} - I_{sd} (e^{qV/kT} - 1) \right\} \quad \dots(14)$$

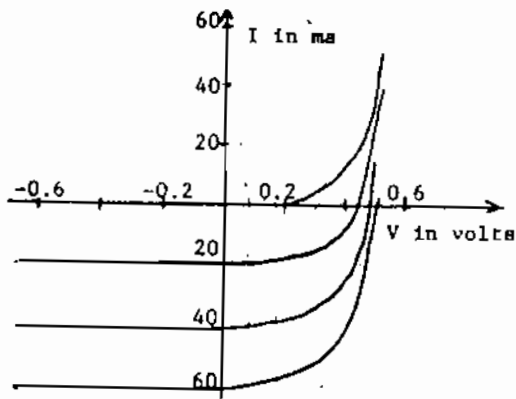
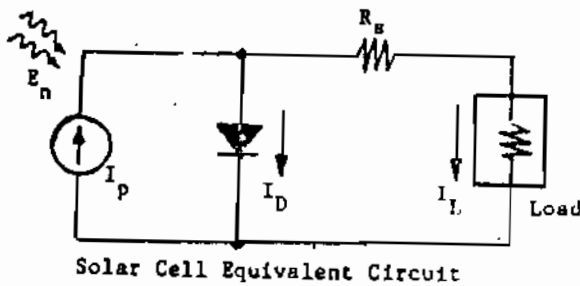


Fig.(9): I-V charectistic for actual junction PV cell for several light intensities.



Solar Cell Equivalent Circuit

Fig.(10): Solar Cell Equivalent Circuit.

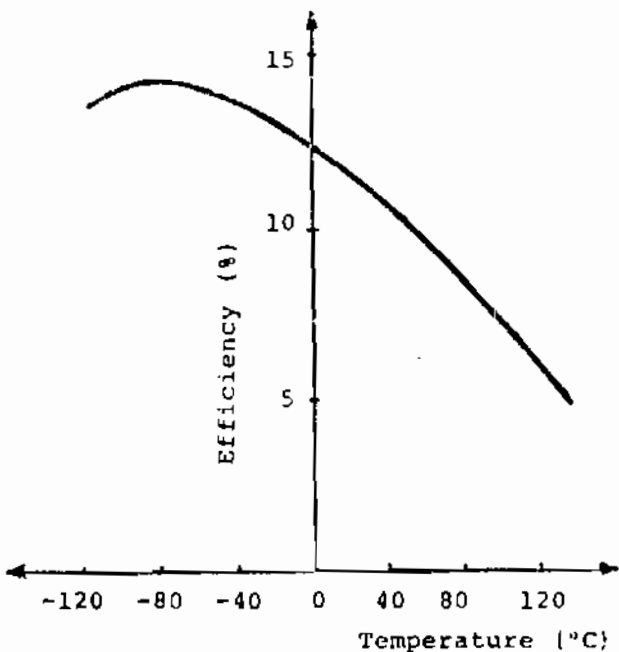


Fig.(11): Varietion of the efficiency with with temperature.

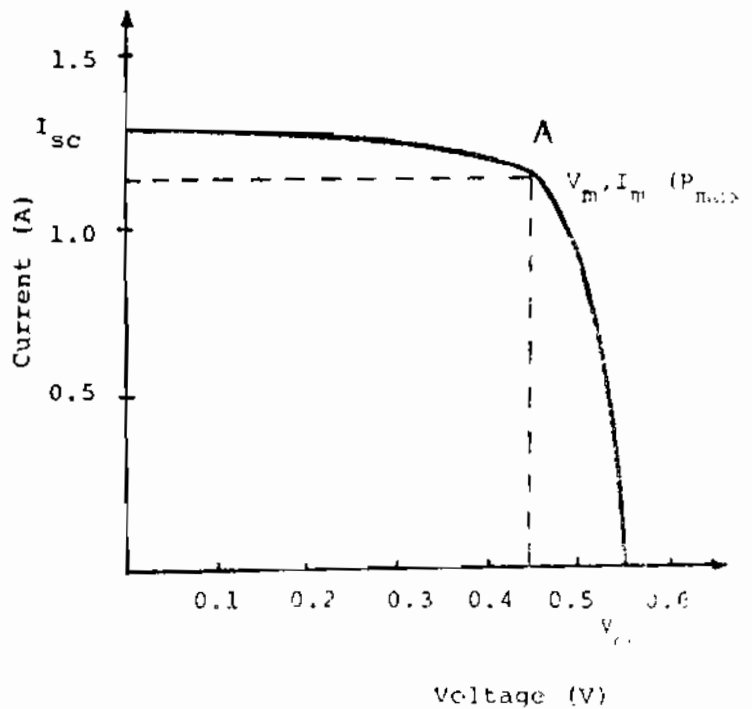


Fig.(12): Maximum efficiency point

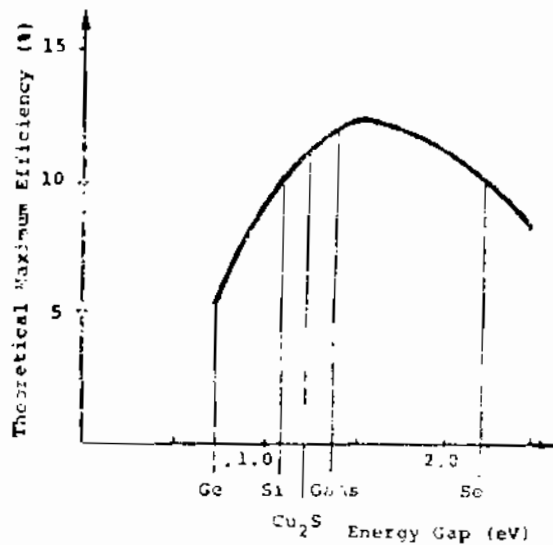


Fig. 13: Variation of the theoretical efficiency with the energy gap (E_g) of the material used for p-n junction solar cells

The maximum power P_m is determined by calculating the corresponding voltage V_{mp} which maximizes P from the condition $dp/dv = 0$.

this leads to $P_m = I_{mp} V_{mp} = (q V_{mp}/KT)(1+q V_{mp}/KT)^{-1} V_{mp} I_{sc}$ (15)

The maximum power point is shown as point A in Fig(12) and P_m is the area of the rectangle within the dashed lines. It is the largest rectangular area that can be included under the characteristic curve. (2)

It could be seen from equations, 1,2....5 that the I-V characteristic and P_m value of the photovoltaic cell is effected by the intensity of light falling on the cell, the temperature and the energy gap of the material of the P-N junction of the cell. The effect of these factors are shown in Fig.(13); from which it could be deduced that the specific capital and operating costs of the P.V. arrays will vary according to the construction and the environmental operating conditions of such cells. From this point of view convenient nomogram analysis is presented here so as to be used as a simplified approach for the solar specific annual energy cost calculations.

As example of which may be illustrated as follows:
Referring to Fig.(14).

N.B. As the total specific annual cost with contain both local and hard currencies, and in order to unify the total specific cost in dollars for our example here, it has been considered that 1 \$ = 1.3 L.E.

Electricity Unit Price:

The key parameter when comparing alternative means of generating electricity for any specific application is the unit energy cost, the cost per kilowatt-hour. Assuming the full annual electrical output of the system is used, the unit energy cost is given by the following relationship.

$$\text{unit energy cost} = (\text{annual capital charges} + \text{annual operating costs}) / \text{total energy output.}$$

This can be expressed as:

$$p = \frac{r \cdot C_{cap} + m \cdot W_p}{\eta_{ave} \cdot P_{in}} \quad \dots (16)$$

where;

- p = unit cost per kWh;
- r = interest plus amortization factor (depends on discount rate and amortization period);
- C_{cap} = total capital cost of system;
- m = specific operation cost, expressed as cost per peak watt installed;
- W_p = total installed peak power in watts;
- η_{ave} = annual average conversion efficiency of system;
- P_{in} = total annual solar energy incident on the array.

As an example, let us consider a 10kWp remote stand-alone system built in Northern cost of Egypt in the late 1980s when photovoltaic module costs are expected to have fallen to about \$ 2.00/W_p and total installed costs for a complete generator system, including battery storage, to be about \$ 5.00/W_p. The total capital cost would thus be \$ 50,000. Assuming a 20 year amortization period and 5% rate of return, the factor r would be 0.0802 and thus the annual capital charges would be \$ 4012. The annual operating cost, including maintenance and insurance, might be of the order of \$ 0.06/W_p and thus the total annual operating cost would be \$ 600. Taking the total area of a 10 kWp array to be 100 square metres, and assuming the installation was at a place where the total annual solar energy incident on the plane of the array was 1750 kWh/m², E_{in} would thus be 175,000 kWh. Based on an annual average conversion efficiency of 7.5%, the total annual energy output would be 13,125 kWh. The unit energy cost would thus be:

$$p = \frac{4012 + 600}{13,125} = \$ 0.35/\text{kWh} \quad \dots (17)$$

0.46 U.S./kWh

It should be noted that the interest rate used in the above example is the real rate of return given by the difference between the cost of money and the inflation rate.

To compare the effect of climatic region data on the cost of the kWh, the same calculations has been repeated for another site in upper Egypt (East oweinat), ca 1500 km south west of Cairo, 450 km west of Aswan. Assuming the same: plant size, P.V. cells cost, system cost, life time, annual operating cost, conversion efficiency and real rate of return; as this site annual energy input reaches about 3000 kWh/m² the unit energy cost would be \$ 0.21/kWh, this gives very competitive prices w.r.t. conventional systems. Another point in favour of the remote sites in upper Egypt in addition to high solar insolation values and longer duration hours is the remoteness factor which adds additional item to the unit energy cost in the case of fossil fired generators due to fuel transport. This item of operational cost increases the fuel cost as much as many folds which again adds to the merits of solar P.V. systems.

It could be seen from the above example that the results obtained for the specific annual cost/kWh are subjected to variations according to the site solar intensity system efficiency, rate of return, photovoltaic system cost \$/W_p, annual operating cost \$/W_p. By the use of the nomogram analysis shown in Fig.(14), Tables (2,3, 4,5,6,7) present the specific annual cost \$/KWH for different sites in Egypt, if the following parametric variations are changed from:

- i) 1750 KWH/m² year (ALX.) to 3000 KWH/m² (Aswan) for solar total annual energy incident on plane of array KWH/m² year.
- ii) 0% to 20% interest rate (20 years amortization period).
- iii) 0.00 to 0.012 annual operating cost \$/W_p.
- iv) \$ 10- \$ 2, Total capital cost of P.V. system \$/W_p.
- v) 10% to 5% annual average conversion efficiency.

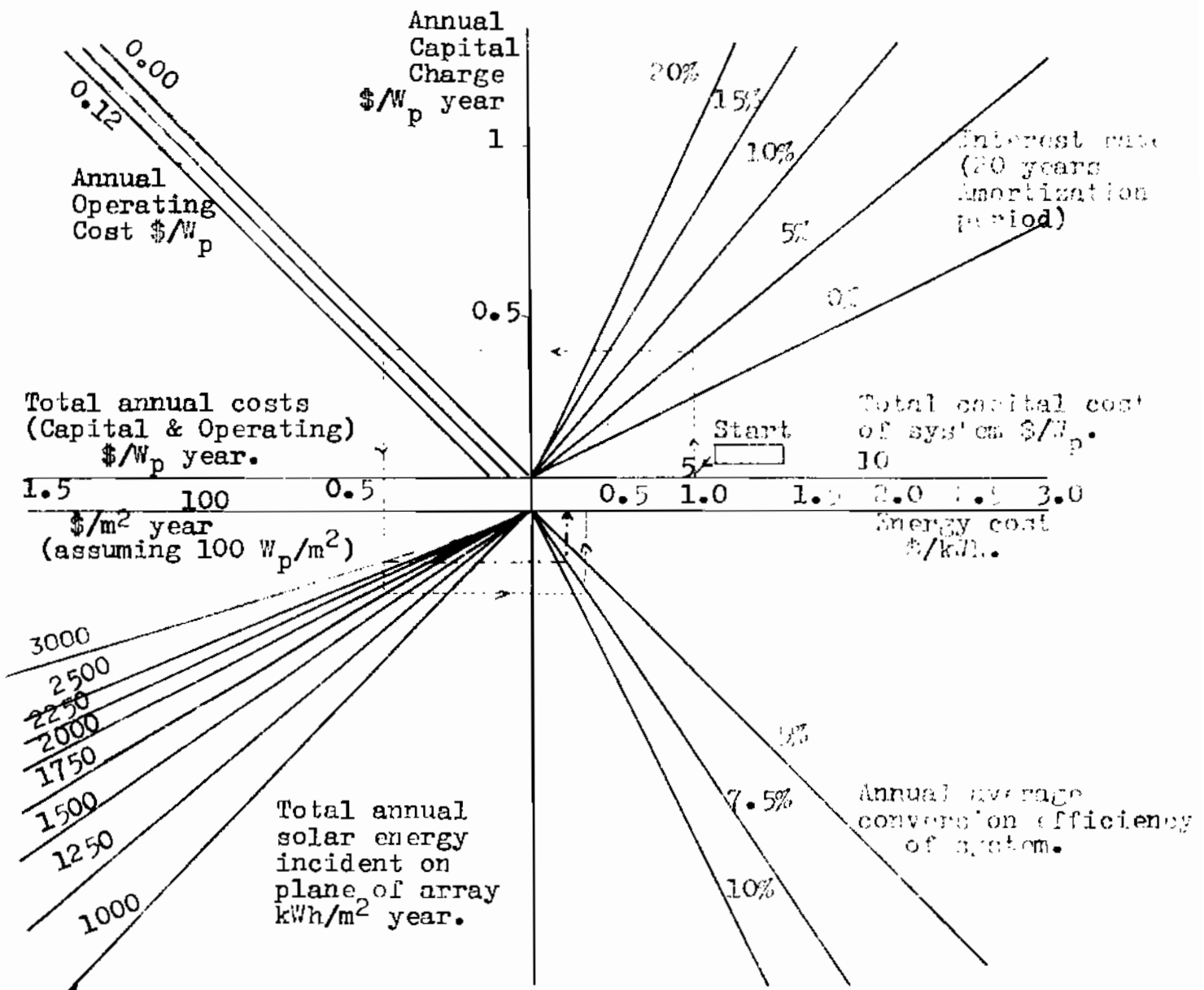


Fig.14 : Simplified approach for calculating unit energy cost.

This simplified approach to photovoltaic system economic analysis is represented graphically in Fig.14, which can be used to derive unit energy cost for different values of capital cost, interest rate, specific operating cost, total incident solar energy and average system conversion efficiency.

The same concept can be applied for wind energy systems taking different average annual wind speeds for different wind machines with different efficiencies and costs.

The next step is to consider the electricity unit cost given by alternative sources for comparison with the photovoltaic system, to see when the break-even points occur. For example, a typical price in Egypt for grid real price of electricity supplied to domestic consumers is \$ 0.00/kWh. A typical price for electricity generated by large (i.e. 2-10 MW) diesel or gas turbine generators (GTs) in remote areas is about \$ 0.20/kWh. These unit prices may be expected to rise at a rate higher than the general inflation rate. In recent years, the differential inflation rate for commercial energy in most countries has been over 10% per annum, but it is generally considered unlikely that such a high rate will persist for much longer. The probable range for the differential inflation rate for electricity supplied from the three sources referred to above (grid, large diesels or GTs, small diesels) is between 5 and 10%.

Thus, whereas the price of photovoltaic systems, and hence the cost of the electricity generated by such systems, is expected to fall in real terms over the next 10-20 years, the cost of electricity from conventional generators is almost certain to rise in real terms over that period. The consequences are illustrated in general terms in Fig.15, which shows that photovoltaic systems in regions with high solar insolation (e.g. southern Egypt) could be competitive with small diesels in remote areas by the late-1980s, with larger diesels and GTs in remote areas by the mid-1990s and with grid supplies by the late-1990s. For places with less solar insolation (e.g. central and northern Egypt), the corresponding break-even dates would be later by some 3-5 years.

Clearly, for specific systems and locations considerably more detailed economic analyses need to be made, but the above simplified approach provides a good indication of the potential for photovoltaics to be competitive with conventional generating systems, including, in time, grid-supplied electricity.

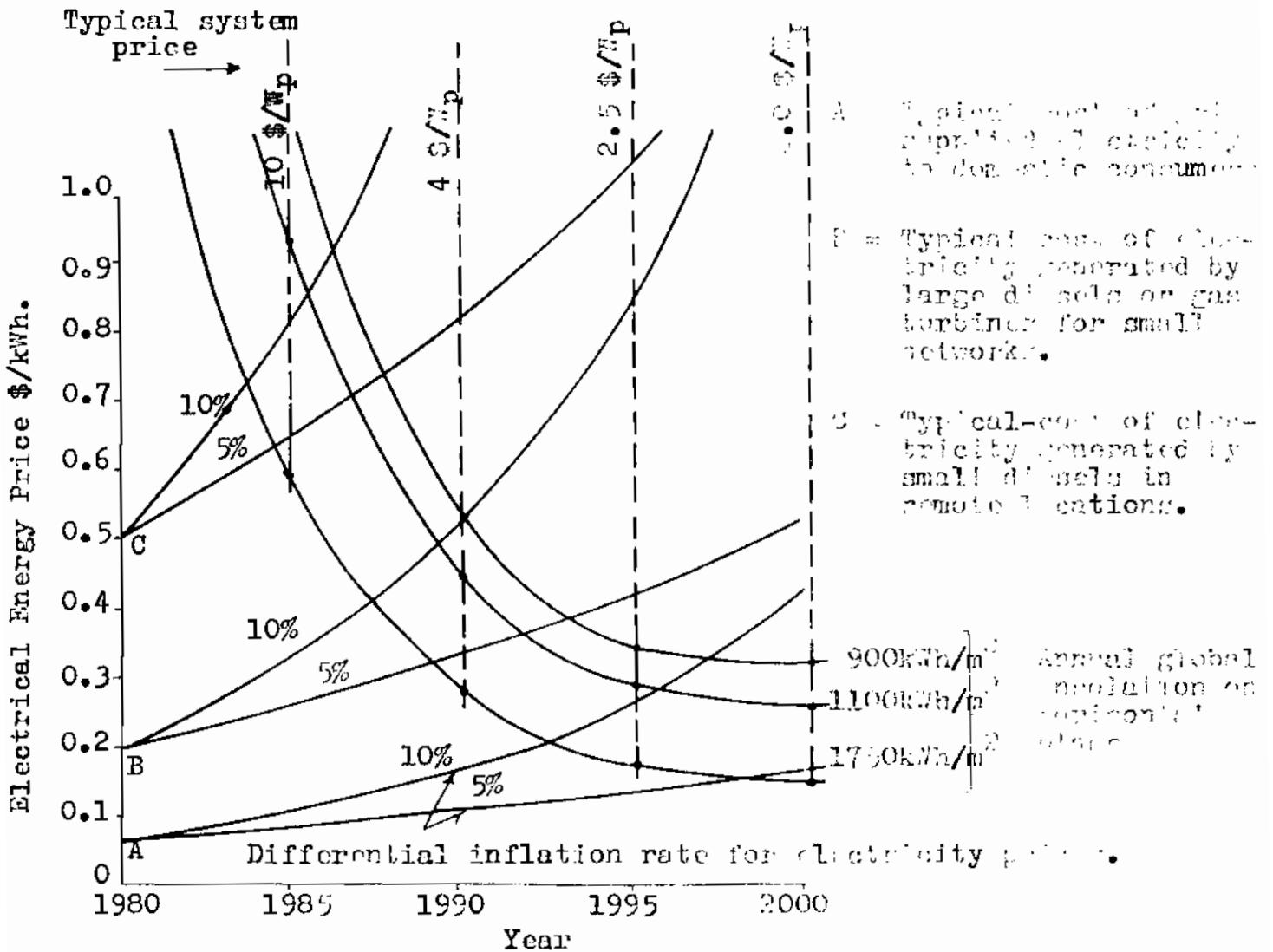


Fig.15 : Photovoltaic system break-even points.

1 \$ U.S. = 1.3 L.E.

CONCLUSIONS

- P.V. systems have good potential to be competitive in the near future with conventional generating systems including grid supplied electricity.
- Photovoltaic systems in the southern parts of Egypt could be competitive with small diesel in remote areas by the late 1980's, with larger diesel and C.T.'s in remote areas by the mid 1990's and with grid supplies by the late 1990's
- The corresponding break even dates for northern Egypt would be later by some 3-5 years.
- Storage batteries are expensive item in the P.V. system, and to secure 100% autonomous system at reasonable price, conventional-back up fossil fired generator or hybrid wind solar systems might be economical solutions according to site characteristics.

NONENCLATURE

- A : Daily Balance
 A_1 : P.V. collector area times efficiency in m^2
 B : Total daily balance
 C_B : Actual battery state of charge.
 C_{BA} : State of charge of the battery allowed.
 $C_{max.}$: Nominal battery size capacity (Ah)
 $C_{min.}$: Minimum state of charge allowed to ensure long life of battery.
 C_{rc} : prescribed state of charge (say 0.5 $C_{max.}$).
 E_A : Energy entering the battery.
 E_D : Energy deficit supplied by conventional energy source.
 E : Daily load demand.
 E_G : Night load demand.
 E_p : Electrical energy output from P.V. array at max. power point ($H A_1$).
 E_s : Energy surplus.
 G_s : Day energy Demand
 G_D : Battery storage capacity in days.
 H : Solar radiation /unit area.
 n : Month index.
 N_{NA} : Night energy demand (Number of days).
 S_m : Solar radiation on the cells in kWh/m^2 .
 η_B : efficiency of power battery.
 η_I : efficiency of power inverter.
 $\eta_{P.C}$: efficiency of power conditioner.
 η_{PT} : efficiency of power tracker.
 N_A : number of days needed to get the deficit condition $C_B = C_{min.}$
 N_D : number of days deficit will be recorded.
 N_C : $N + N_D$
 ΔC_{BA} : Change of state of charge (day)
 ΔC_{BH} : Change of state of charge (night).
 A_{IP} : normalizing unit = $\frac{\text{daily average power demand}}{C_{PT} (I_p \cdot V / \eta)}$
 S_D : $= \frac{(C_{max} - C_{min}) \eta_I \eta_C}{E_G + E_{II}}$
 Number of days, the battery can feed load without the support of the PV energy.
 A_1/A_{1p} : size of P.V. plant in normalized form.

REFERENCES:

-
1. Joseph A. Merrigan - Sunlight to Electricity - The MIT Press 1975.
 2. W. Palz - Solar Electricity - UNESCO - Butterworths 1978.
 3. M. Giuffrida - Courses on Photovoltaic Solar Devices - SOGESTA, 1980.
 4. M. Giuffrida - Use of photovoltaic Power Supply Unit for Cathodic Protection - SOGESTA, Italy, 1980.
 5. Jensen, J. Perram, C. Dell, R.M., Batteries for Solar electricity, 2nd E.C. Photovoltaic energy conference, proceedings of the international conference held at Berlin (West), April 1979.